THE WEST EUROPE PRESSURE ANOMALY (WEPA): A SIMPLE SEA-LEVEL-PRESSURE BASED CLIMATE INDEX CONTROLLING WINTER WAVE HEIGHTS ALONG THE WESTERN COAST OF EUROPE FROM PORTUGAL TO UK (36-52°N)

Bruno Castelle[1], Guillaume Dodet[2], Gerd Masselink[3] and Tim Scott[3]

Abstract

A method based on a 66-year numerical weather and wave hindcast is developed to optimize a climate index based on the sea level pressure (SLP) that best explains winter wave height variability along the coast of western Europe, from Portugal to UK (36–52°N). The resulting so-called Western Europe Pressure Anomaly (WEPA) is based on the sea level pressure gradient between the stations Valentia (Ireland) and Santa Cruz de Tenerife (Canary Islands). WEPA outscores by 25–150% the other leading atmospheric modes in explaining winter-averaged significant wave height. WEPA is also the only index capturing the 2013/2014 extreme winter, characterised by a succession of large storms throughout the winter season and causing widespread coastal erosion and flooding in Western Europe. More detail can be found in the recently published study of Castelle et al. (2017).

Key words: wave climate, winter extremes, interannual variability, Western Europe, coastal hazards

1. Introduction

Winter and extreme coastal wave climate variability is a recent and important topic in climate studies and it becomes increasingly important to link extreme wave energy arriving locally at the coast to large-scale oceanic and atmospheric variability (e.g. Perez et al., 2014). Extreme coastal wave climate and coastal hazards are strongly affected by large-scale climate patterns of atmospheric and oceanic variability on interannual and longer timescales. For instance, Barnard et al. (2015, 2017) show that the El Nino–Southern Oscillation can cause extreme coastal erosion and flooding across the Pacific. Given that changes in extreme wave climate have the potential to cause dramatic change in the equilibrium state of beaches (Masselink et al., 2016a), it is important to better understand the primary atmospheric patterns and climate indices controlling the variability of winter wave activity.

The North Atlantic Oscillation (NAO) has long been known to affect climate variability in the Northern Hemisphere (Hurrell, 1995) and, as a result, the wave climate arriving at the west coast of Europe (e.g., Bacon and Carter, 1993; Dodet et al., 2010). Climate indices can be computed based on sea level pressure (SLP) measurements located within well-known atmospheric structures. The NAO was formerly computed (Hurrell, 1995) as the SLP difference between the Iceland (ICE in Fig. 1a) and a southern station (Lisbon, Azores, or Gibraltar; LIS, AZO and GIB in Fig. 1a). This gradient was chosen to capture the SLP difference variability between the Azores high and the Icelandic low (Fig. 1a), which is the primary atmospheric pattern generating waves towards west coast of Europe (Fig. 1b). The influence of the NAO on waves along the Atlantic coast of Europe is particularly strong in the winter months (e.g., Bromirski and Cayan, 2015). A number of studies investigated how the NAO impacts shoreline change and coastal behaviour, e.g., in UK (Masselink et al., 2014) and France (Robinet et al., 2016), showing that the NAO can explain a small, but significant, amount of the observed coastal variability. An explanation for this is that while the NAO has a major impact on the Atlantic winter wave height in the northern sector (NW of

[1]   CNRS/Unv. Bordeaux, UMR EPOC, Allée Geoffroy Saint-Hilaire, France. bruno.castelle@u-bordeaux.fr
[2]   LETG-Brest Geomer UMR 6554 CNRS, Institut Universitaire Europeen de la Mer (UBO), Plouzane, France. guillaume.dodet@univ-brest.fr
[3]   Coastal Processes Research Group, School of Biological and Marine Sciences, Plymouth University, UK. gerd.masselink@plymouth.ac.uk; timothy.scott@plymouth.ac.uk

the British Islands), its influence is more subtle at more southern latitudes (UK, France, Spain, and Portugal, Dupuis et al., 2006). In these regions, winter waves are more affected by other leading atmospheric modes in the North Atlantic, namely, the East Atlantic (EA) and Scandinavia (SCAND) patterns (Shimura et al., 2013). Contrary to NAO, these climate indices are typically computed through the principal empirical orthogonal function (EOF) of SLP derived from numerical weather hindcast to give a physically based expression of atmospheric structure (e.g., Rogers, 1981). The absence of a climate index specific to the Atlantic coast of mid-southern Europe and the resulting lack of understanding of the major atmospheric control on winter wave climate along this coast is a major drawback. An example is the winter 2013/2014 that was characterized by extreme winter wave activity (Masselink et al., 2016a) and sea level events (Haigh et al., 2016) along the Atlantic coast of Europe, with the largest winter-averaged wave energy arriving at the coast in middle to southern latitude, i.e., 55°N–38°N, over at least the last 67 years (Masselink et al., 2016a). This 2013/2014 winter, which caused unprecedented coastal erosion in many locations from western Europe down to Morocco (e.g., Castelle et al., 2015; Suanez et al., 2015; Masselink et al., 2016a, 2016b; Crapoulet et al., 2017), was not captured by any of the above mentioned climate indices. From the perspective of coastal hazards, climate indices are therefore also relevant if they can explain extreme wave activity (numerous storms as opposed to one single severe storm, which is critical to flooding, cliff failure, and beach erosion (e.g., Menendez et al., 2008; Ruggiero et al., 2010; Barnard et al., 2011).
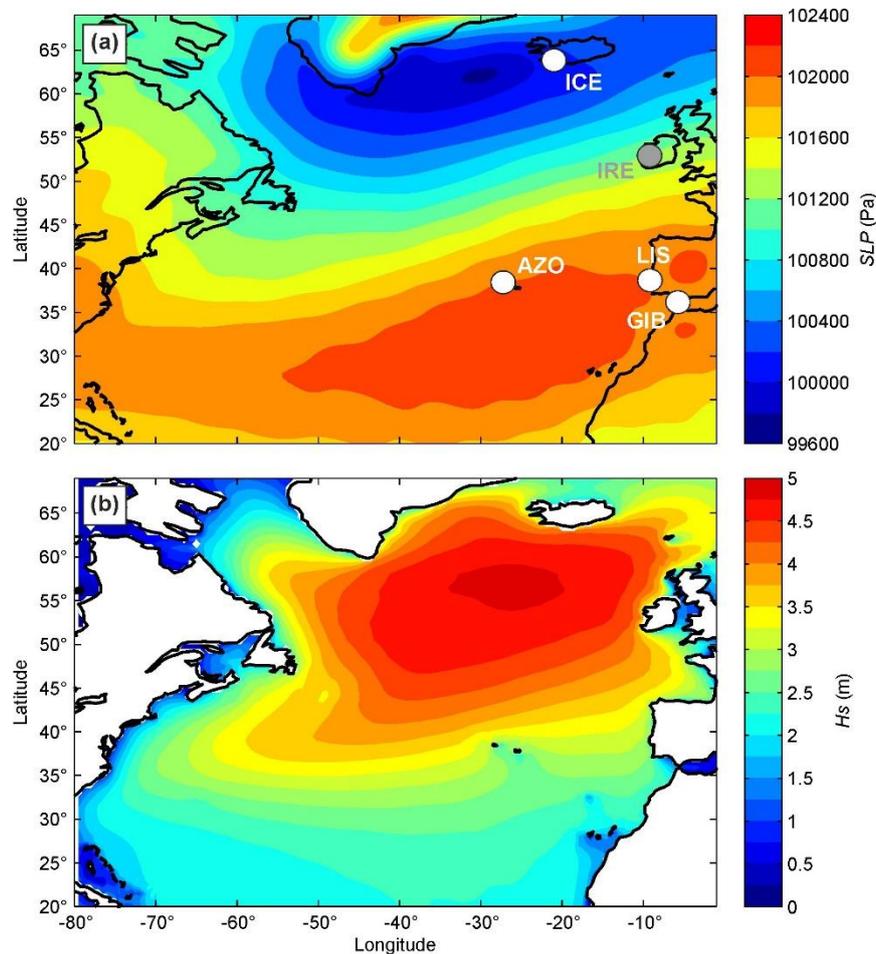
Figure 1. Winter-averaged (DJFM, 1950-2016) (a) SLP (Pa) and (b) *Hs* (m) in the North Atlantic Ocean. In panel (a) the SLP stations from which the NAO is typically computed are indicated (ICE: Iceland; AZO: Azores; LIS: Lisbon; GIB: Gibraltar). Their location in the vicinity of the center of the pressure systems was chosen to capture to capture the SLP difference variability between the Azores high and the Icelandic low. In contrast, the Ireland station that will be objectively picked up to compute our new climate index is located in the land area with maximum SLP gradient.

Climate indices can be computed through the principal empirical orthogonal function (EOF) of surface pressure derived from numerical weather hindcast to give a physically based expression of atmospheric structure (e.g., Rogers, 1981). Alternatively, indices based on sea level pressure (SLP) measurements can also be computed based on well-known atmospheric structures if relevant land-based measurements exist (e.g., the NAO as the SLP difference between ICE and a southern station, Hurrell, 1995). EOF- and SLP-based NAO indices generally show very good agreement (Hurrell and Deser, 2009). However, compared to EOF-based indices that need reliable numerical hindcast of large-scale SLP patterns, SLP-based indices using two SLP stations have the advantage that they can be calculated back to the early 1900s, or even 1800s, as measured weather data from more than 100 years are not uncommon across the world (Trenberth and Paolino, 1980; Jones et al., 2013).

In this paper, we develop a new SLP-based climate index that acts as a primary control on winter waves along the Atlantic coast of Europe. Here SLP-based indices are preferred to EOF-based indices that need reliable numerical hindcast of large-scale SLP patterns. Previous studies systematically developed or used climate indices based on their atmospheric expression to further address their influences on, for instance, rainfall, temperature, or wave climate. Instead, here the index is reverse engineered from the end product, namely, winter wave height along the west coast of Europe, as large wave heights are the primary cause of coastal hazards. The optimal SLP gradient that best explains the observed variability of winter wave activity is objectively searched from a 66 year numerical weather and wave hindcast. It will be shown that our new index explains between 40% and 90% of the observed winter-averaged wave height variability from southern Ireland down to Portugal, where all the other indices explain at best 40% and that it also captures the extreme winter of 2013/2014. For more detail and a description of the atmospheric expression of this new climate index, the reader is referred to Castelle et al. (2017).

2. Methods

2.1. *Data and model outputs*

The data and method used are described in detail in Castelle et al. (2017). In short, 6-hourly SLP and 10-m wind ($\vec{u}_{10}$) fields (2.5°x2.5°) were downloaded/obtained from the National Centers for Environmental Prediction (NCEP) / National Center for Atmospheric Research reanalysis project (Kalnay et al., 1996), while EOF-based monthly teleconnection indices NAO, EA, and SCAND were downloaded from the National Oceanic and Atmospheric Administration (NOAA) Climate Prediction Center (www.cpc.ncep.noaa.gov). Following the modelling strategy validated in Masselink et al. (2016a), the spectral wave model Wave Watch III V4.18 (Tolman, 2014) was implemented on a 0.5° resolution grid covering the North Atlantic Ocean (80°–0°W; 0°–70°N) forced with the 6-hourly wind fields $\vec{u}_{10}$.

2.2. *Method*

Hereafter, we address winter (December, January, February, and March - DJFM) averages of wave and atmospheric variability from 1950 to 2016 (66 winters). Virtual climate indices were computed as the normalized SLP-gradient anomaly between any grid point pairs within the whole domain (80°–0°W; 0°–70°N). Winter averages of climate indices, grid point significant wave height *Hs*, and their 90%, 95%, and 99% exceedance values ($Hs_{90\%}$, $Hs_{95\%}$, and $Hs_{90\%}$, see Figure 2 for their spatial distribution averaged over the 66 winters), $\vec{u}_{10}$, and SLP were computed. The relationship between all possible virtual climate indices and winter-averaged *Hs* at 6 virtual wave buoys along the entire Atlantic coast of Europe from Scotland in the north to Portugal in the south (Figure 3: SC: Scotland; IR: Ireland; BR: Brittany; BI: Biscay; GA: Galicia; PT: Portugal) was studied computing the correlation coefficient *R* between the normalized time series of winter-averaged *Hs* and all virtual climate indices. For each virtual buoy along the Atlantic coast of Europe, the pair of virtual land-based SLP stations that gave the highest correlation *R* was used to define the optimal climate index to explain the variability of winter-averaged *Hs* at that location. Finally, storm tracks were computed using the algorithm described in Murray and Simmonds (1991). This method is based on the local maxima in relative vorticity, rather than local pressure minima, as the former was shown

to also identify small-scale pressure systems and was further validated in the North Atlantic Ocean (Pinto et al., 2005).
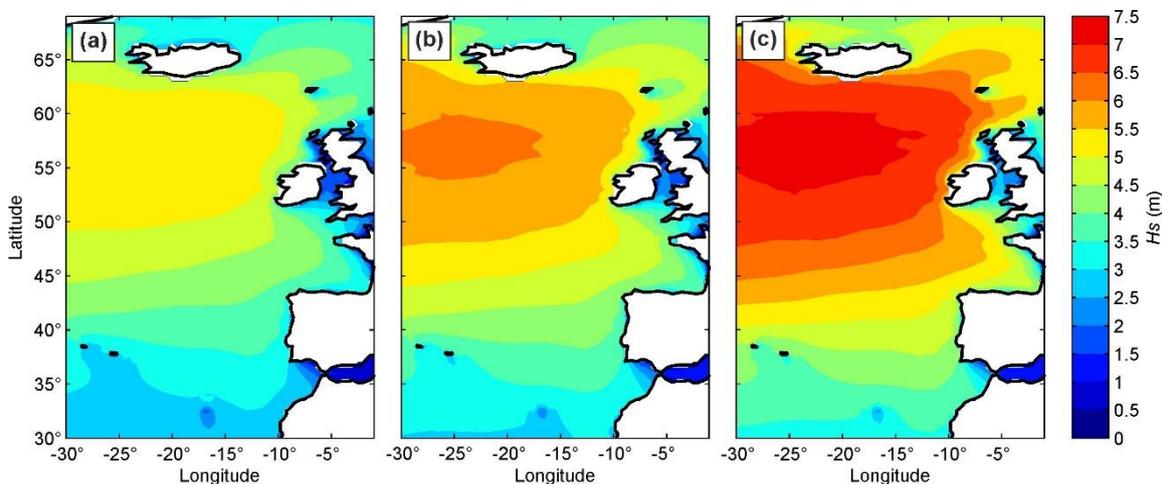
Figure 2. Winter-averaged (DJFM, 1950-2016) of (a) $Hs_{90\%}$, (b) $Hs_{95\%}$ and (c) $Hs_{90\%}$.

3. Results and Discussion

Figure 3 shows that the largest amount of winter-averaged Hs variability at the Scottish buoy (SC) is explained by the SLP-based Iceland-Lisbon definition of the NAO, which shows slightly better correlation than using the Iceland-Gibraltar definition. In contrast, the largest amount of winter-averaged Hs variability at all the other buoys (except PT) is explained by the anomaly in SLP gradients between Ireland and various southern locations (Azores, Canary Islands, Spain, or France), with systematically $R > 0.89$ (Castelle et al., 2017). Of note, while Figure 3 displays the optimal land-based SLP gradients, some other land-based SLP gradients also show very good skill. For instance, the optimal SLP gradient for the BI (Bay of Biscay) buoy is Ireland-Azores ($R = 0.92$), but the SLP gradient Ireland-Canary Islands also shows very good skill ($R = 0.86$). Similarly, the NAO (Iceland-Lisbon gradient definition) shows very good skill ($R = 0.79$) for the IR buoy, although it is outscored by a SLP gradient between Ireland and Brittany (R = 0.9, Castelle et al., 2017).

In order to develop a single, relevant, climate index, we searched for an index that skilfully explains the winter-averaged Hs along the entire Atlantic coast of Europe. However, the atmospheric patterns controlling wave heights at the southern and northern latitudes of the west coast of Europe are significantly different and the NAO is known to strongly control winter height in the northern regions. Therefore, we searched for the optimal SLP gradient that, on average, shows the best correlation with the four southern buoys (black line gradient in Figures 3). Results show that the variability of winter-averaged Hs is strongly controlled by an optimal SLP gradient between Ireland and Canary Islands. It is important to note that the optimal land-based SLP gradient showing the best correlation averaged over the six buoys is also Ireland-Canary Islands, although poor correlation is found at the northern latitudes. Hereafter, this optimal climate index is referred to as the Western Europe Pressure Anomaly (WEPA, Castelle et al., 2017) and is calculated from the daily measured (not hindcast) SLP at Valentia station (Ireland) and Santa Cruz de Tenerife, Canary Island (Spain). The fact that taking Ireland as the northern station rather than Iceland is critical to explain the winter wave activity variability, particularly in southern Europe, is further emphasized in Figure 4.
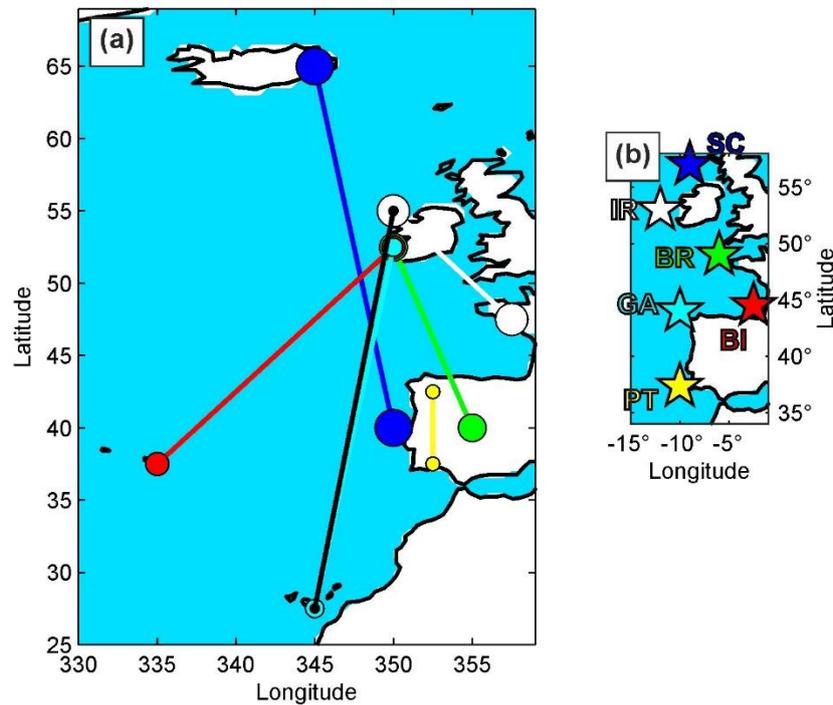
Figure 3. Simulated optimal winter-averaged (DJFM) SLP gradients from (a) virtual stations containing land within the corresponding 2.5° × 2.5° cell, which explain the largest amount of variability of winter-averaged Hs at (b) six virtual wave buoys along the west coast of Europe. SC: Scotland; IR: Ireland; BR: Brittany; BI: Biscay; GA: Galicia; PT: Portugal. The buoys considered for each gradient are given by the colour code, and the black gradient in Figures 1a and 1b indicates the optimal pressure gradient combining the four southern buoys BR, BI, GA, and PT.
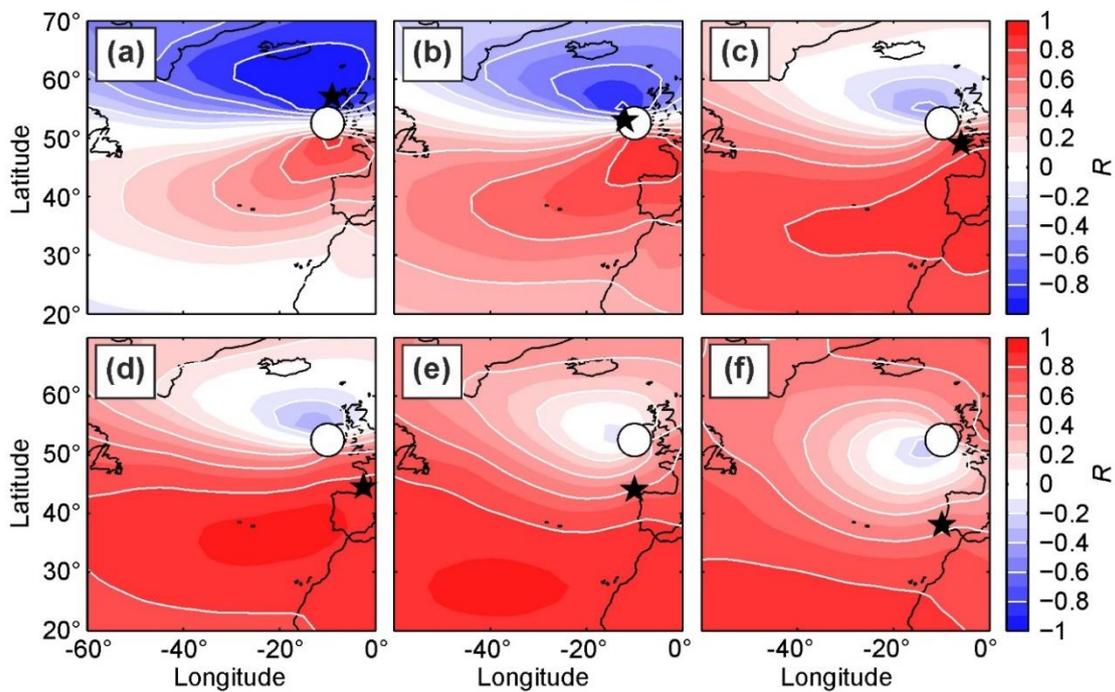
Figure 4. Spatial distribution of correlation *R* between the winter-averaged (DJFM) *Hs* at the virtual buoy (black star) and the climate index defined as the normalized SLP difference between Ireland (white circle) and all possible grid points within the domain. Results show that, for most of the southern buoys, Canarias are in the vicinity of the area of maximum *R*.

Figure 5 shows the spatial distribution of the correlation between the winter-averaged *Hs* and four climate indices, namely, NAO, EA, SCAND, and our new index WEPA. The spatial distribution for SCAND shows poor correlation found across the whole East Atlantic (Figure 5b). In line with earlier studies (e.g., Dodet et al., 2010; Shimura et al., 2013; Bromirski and Cayan, 2015), the NAO is found to have a strong influence on the winter-averaged *Hs* at the northern latitudes (Figures 5a). This influence dramatically decreases south of 52°N. In contrast, the EA shows better correlation south of 52°N, although the correlation *R* along the coast is systematically below 0.65 (Figure 5c), meaning that EA explains at best approximately 40% of the observed winter-averaged *Hs* variability. Figures 5d shows the same analysis for our new climate index WEPA. Clearly, the correlation with winter-averaged *Hs* across the Atlantic coast of Europe south of 52°N is greatly increased (*R* > 0.8), with even areas showing *R* > 0.9–0.95 (*e.g.*, *R* = 0.91 at Galicia buoy GA, Castelle et al., 2017).
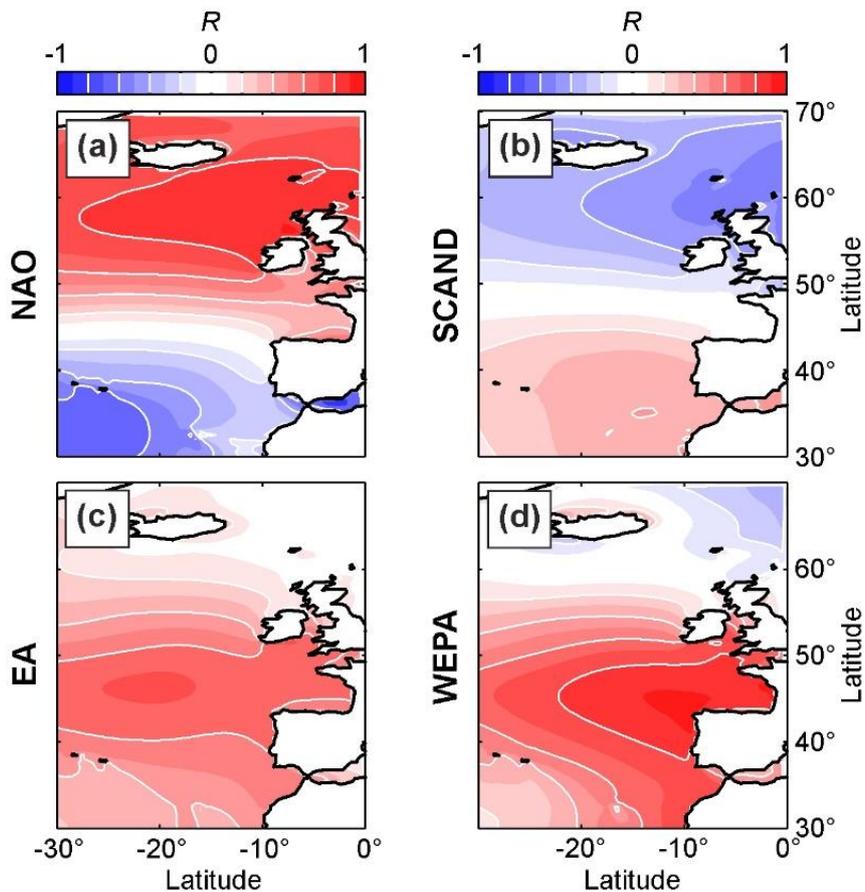
Figure 5. Spatial correlation of the winter (DJFM)-averaged *Hs* against the winter-averaged (a) NAO, (b) SCAND, (c) EA and (d) against our new WEPA index computed as the normalized SLP difference measured between station Valentia (Ireland) and station Santa Cruz de Tenerife (Canary Islands, Spain).

In addition, it is important to note that only WEPA captures the 2013/2014 winter that was characterized by extreme wave activity along the Atlantic coast of Europe (Masselink et al., 2016a, Figure 6). This is further emphasized by the spatial distribution of the correlation between the winter-averaged $Hs_{95\%}$ and the same three climate indices (not shown, see Castelle et al., 2017). Therefore, WEPA captures both the temporal (2013/2014 winter) and spatial variability of extreme wave energy, which is critical from the perspective of coastal hazards.

The relevance of the WEPA for the west coast of Europe is further emphasized in Figure 7 that displays the spatial distribution of the optimal climate indices to explain the winter wave climate within the NE Atlantic. The optimal climate index is defined as the index with the highest R^2 associated with the local winter-

averaged *Hs*. Here we now switch from R to R^2 both to address the amount of variability explained by the index and to account for negative correlations. Disregarding the WEPA the two optimal climate indices explaining winter-averaged *Hs* along the Atlantic coast of Europe north and south of 52°N are clearly NAO and EA, respectively (Figure 7a). This corroborates the results of Shimura et al. (2013) who included nine teleconnection index in their study. Including the WEPA, Figure 7b shows that WEPA largely outscores the other indices along the Atlantic coast of Europe south of 52°N. Compared to EA, WEPA increases the explanation of the winter-averaged *Hs* variability by 25–150% (see the large increase in R^2 in Figure 8). This improvement is even better when considering extreme wave events with, for instance, an increase for $Hs_{99\%}$ exceeding 200% along most of the Spanish and Portuguese coasts (Castelle et al., 2017).
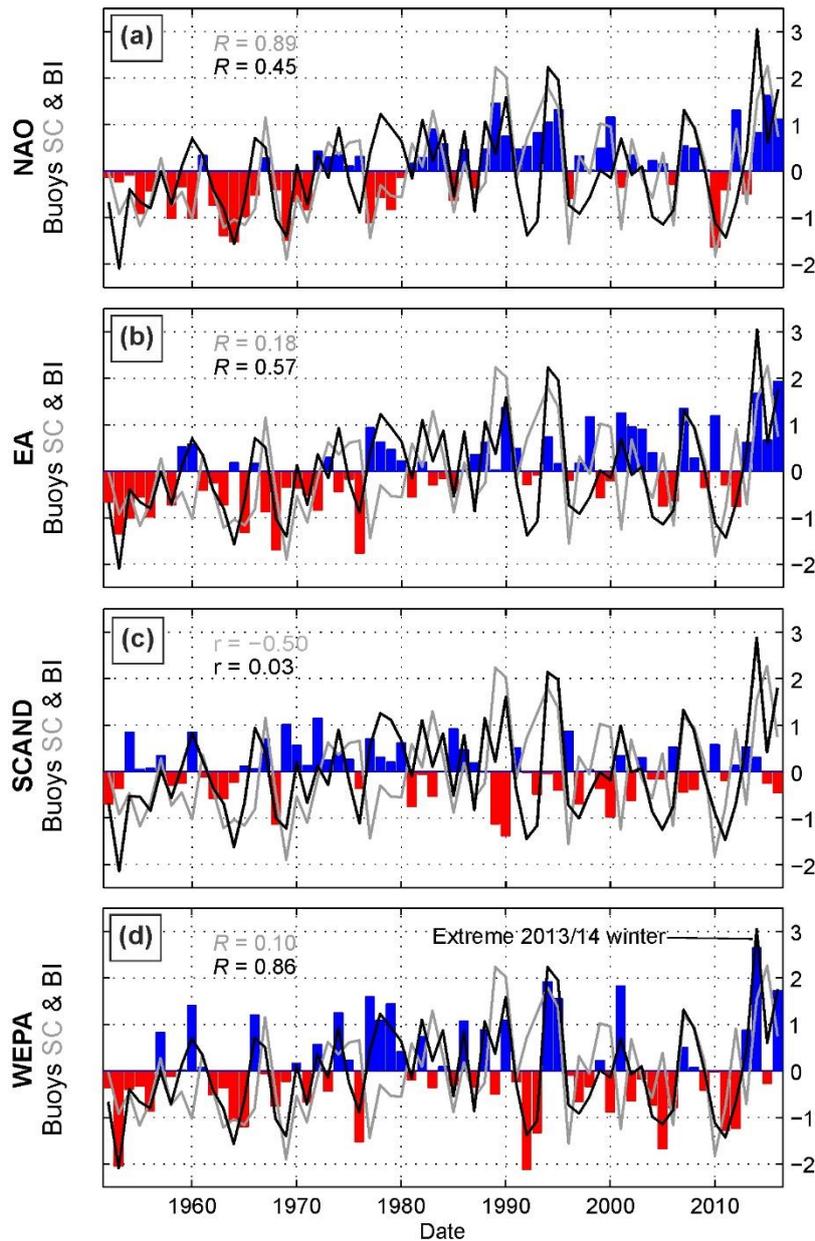
Figure 6. Time series the winter-averaged (a) NAO, (b) EA, (c) SCAN and (d) our new WEPA index computed as the normalized SLP difference measured between station Valentia (Ireland) and station Santa Cruz de Tenerife (Canary Islands, Spain) with superimposed normalized winter-averaged Hs simulated at the buoys SC (Scotland, black) and BI (Biscay, grey) with corresponding correlation coefficient *R*.
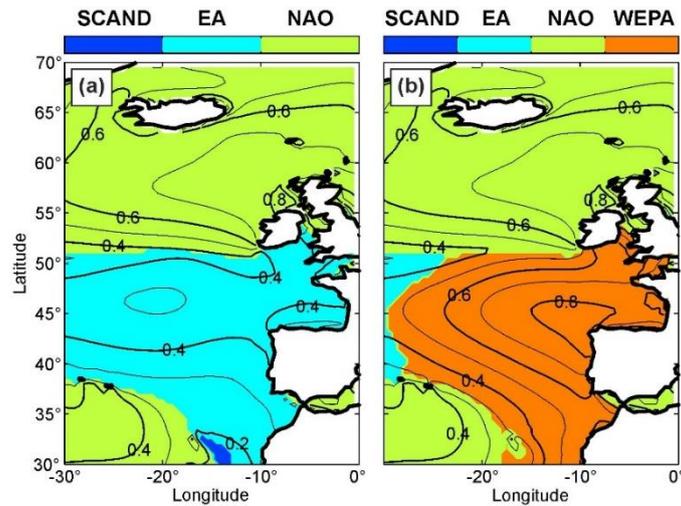
Figure 7. Spatial distribution of optimal climate indices explaining the largest variability of local winter-averaged *Hs* (DJFM) ignoring (a) and accounting (b) for our new WEPA climate index computed as the normalized SLP difference measured between station Valentia (Ireland) and station Santa Cruz de Tenerife (Canary Islands, Spain). The corresponding regression coefficient R^2 contoured in the background of both panels.
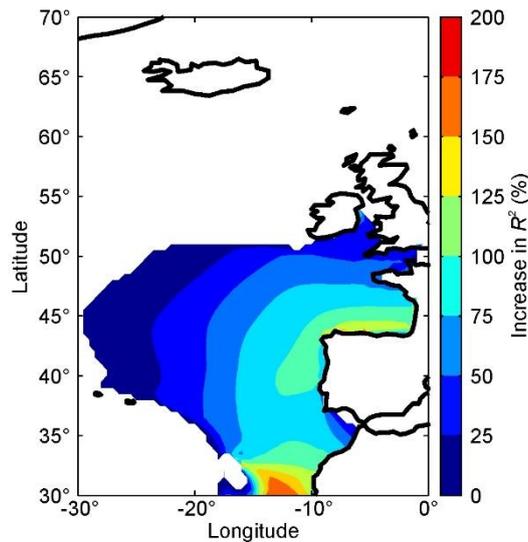
Figure 8. Spatial distribution of the increase (%) in R^2 including the WEPA as a climate index in the NE Atlantic, in the predictability of winter-averaged *Hs*.

To further understand the control of WEPA on winter wave climate along the Atlantic coast of Europe, Castelle et al. (2017) provided physical insight into the atmospheric phenomenon for both the NAO and the WEPA, by looking at the mean Hs, mean SLP and storm tracks during the five winters associated to the lowest (resp, largest) NAO and WEPA phases. The authors showed that the WEPA can be interpreted as a southward shifted NAO, although the indices WEPA and NAO are not correlated ($R = 0.08$). In short, the positive phase of WEPA reflects intensified latitudinal SLP gradient in the NE Atlantic that drives increased W-SW winds around 45∘ associated with severe storms, many eventually passing over UK, which funnel high-energy waves toward Western Europe.

It is relevant to address in more details the interannual variability of the climate indices controlling winter wave activity along the west coast of Europe. A wavelet analysis of NAO and WEPA is shown in Figure 9 to decompose both climate indices at a given time and at a given time scale of variability. In essence, this

enables both the detection of the dominant temporal modes of variability and how these modes vary in time. Results show that, while the NAO does not shown strong evolution in winter mean variability (Figure 9a), WEPA shows a strong increase in interannual variability on the timescales of 5-7 years since the early 90s. This change in temporal variability and resulting increase in extreme winter occurrence (e.g. winter 2013/2014) needs to be explored further.
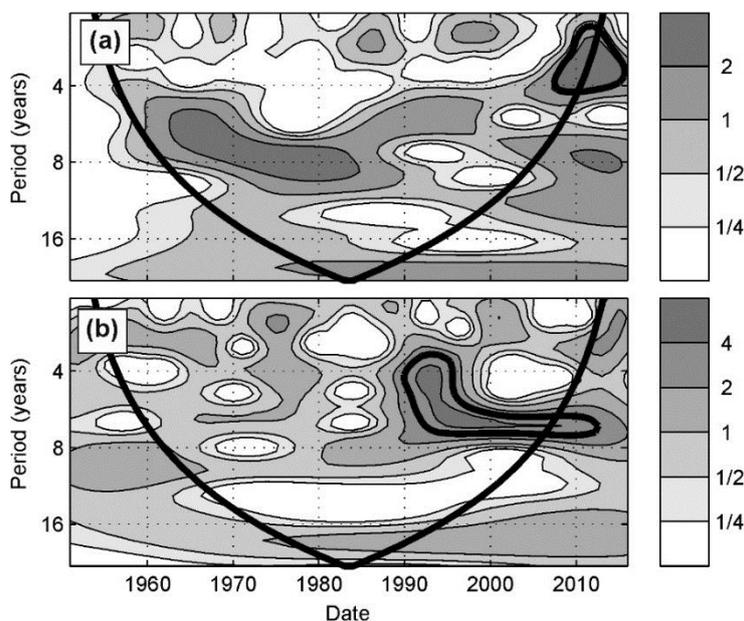
Figure 9. Wavelet spectra of winter (a) NAO and (b) WEPA from 1951 to 2016. In each panel, the wavelet power has been normalized with the variance in NAO and WEPA, respectively, with the 5% significance level against red noise shown as the bold solid contours and the bold dotted curves depicting the cone of influence beyond which edge effects become important.

4. Conclusions

A generic method using numerical weather and wave hindcast was developed to identify the optimal SLP-based climate index explaining winter wave activity along the Atlantic coast of Europe spanning 1950–2016. The resulting so-called Western Europe Pressure Anomaly (WEPA) index is based on the normalized SLP difference measured between the stations Valentia (Ireland) and Santa Cruz de Tenerife (Canary Islands, Spain). Complementary to the NAO that controls winter-averaged Hs in the NW of the British Island (>52°N), our new index WEPA explains between 40% and 90% of the observed winter-averaged Hs variability along the Atlantic coast of Europe southward of 52°N. WEPA largely outscores the SCAND and EA indices, which are often argued as the primary control of winter wave activity in this region. WEPA is also the most relevant index to capture extreme winter wave activity both spatially and temporally, like for the extreme 2013/2014 that caused severe erosion along the Atlantic coast of Europe. We therefore anticipate that the WEPA index is critical to understand coastal hazards in Western Europe.

the NCEP Reanalysis data provided by the NOAA/OAR/ESRL PSD. The wavelet computations in this paper were based on Matlab software developed by Aslak Grinsted and co-workers (version wtc-r14, available from http:// www.pol.ac.uk/home/research/waveletcoherence/). The winter time series of WEPA and WW3 outputs can be provided on demand to B.C. (Bruno.castelle@u-bordeaux.fr) and G.D. (guillaume.dodet@univ-brest.fr), respectively.

References

Bacon, S., Carter, D. J. T., 1993. A connection between mean wave height and atmospheric pressure gradient in the North Atlantic. *Int. J. Climatol*., 13(4): 423–436, doi:10.1002/joc.3370130406.

Barnard, P. L., Allan, J., Hansen, J.E., Kaminsky, G.M., Ruggiero, P., Doria, A., 2011. The impact of the 2009-10 El Niño Modoki on U.S. West Coast beaches. *Geophys. Res. Lett*., 38: L13604, doi:10.1029/2011GL047707.

Barnard, P. L., et al., 2015. Coastal vulnerability across the Pacific dominated by El Nino/Southern Oscillation. *Nat. Geosci*., 8(10): 801–807, doi:10.1038/ngeo2539.

Barnard, P. L., et al., 2017. Extreme oceanographic forcing and coastal response due to the 2015-2016 El Nino. *Nat. Commun*., 8: 14365, doi:10.1038/ncomms14365.

Bromirski, P. D., Cayan, D.R. 2015. Wave power variability and trends across the North Atlantic influenced by decadal climate patterns. *J. Geophys. Res. Oceans*, 120: 3419–3443, doi:10.1002/2014JC010440.

Castelle, B., Marieu, V., Bujan, S., Splinter, K.D., Robinet, A., Senechal, N., Ferreira, S., 2015. Impact of the winter 2013–2014 series of severe Western Europe storms on a double-barred sandy coast: Beach and dune erosion and megacusp embayments. *Geomorphology*, 238: 135–148.

Castelle, B., Dodet, G., Masselink, G., Scott, T., 2017. A new climate index controlling winter wave activity along the Atlantic coast of Europe: The West Europe Pressure Anomaly. *Geophys. Res. Lett*., 44, doi:10.1002/2016GL072379.

Crapoulet, A., Héquette, A., Marin, D., Levoy, F., Bretel, P., 2017. Variations in the response of the dune coast of northern France to major storms as a function of available beach sediment. *Earth Surf. Process. Landforms*, doi:10.1002 /esp/4098.

Dodet, G., Bertin, X., Taborda, R., 2010.Wave climate variability in the North-East Atlantic Ocean over the last six decades. *Ocean Modell*., 31(3–4): 120–131.

Dupuis, H., Michel, D., Sottolichio, A., 2006. Wave climate evolution in the bay of Biscay over two decades. *J. Mar. Syst*., 63(3–4): 105–114.

Haigh, I. D., Wadey, M. P., Wahl, T., Ozsoy, O., Nicholls, R. J., Brown, J. M., Horsburgh, K., Gouldby, B., 2016. Spatial and temporal analysis of extreme sea level and storm surge events around the coastline of the UK. *Sci. Data*, 3, 160107, doi:10.1038/sdata.2016.107.

Hurrell, J. W., 1995. Decadal trends in the North Atlantic Oscillation: Regional temperatures and precipitation. *Science*, 269(5224): 676–679, doi:10.1126/science.269.5224.676.

Hurrell, J. W., Deser, C., 2009. North Atlantic climate variability: The role of the North Atlantic Oscillation. *J. Mar. Syst*., 78(1): 28–41.

Jones, P. D., Osborn, T. J., Briffa, K. R. 2013. Pressure-based measures of the North Atlantic Oscillation (NAO), a comparison and an assessment of changes in the strength of the NAO and its influence on surface climate parameters, In *The North Atlantic Oscillation: Climatic Significance and Environmental Impact*, edited by J. W. Hurrell and others, pp. 1–35, AGU, Washington, D. C., doi:10.1029/134GM01.

Kalnay, E., et al., 1996. The NCEP/NCAR 40-year reanalysis project, Bull. *Am. Meteorol. Soc*., 77(3): 437–471.

Masselink, G., Austin, M., Scott, T., Poate, T., Russell, P., 2014. Role of wave forcing, storms and NAO in outer bar dynamics on a high-energy, macro-tidal beach. *Geomorphology*, 226, 76–93.

Masselink, G., Castelle, B., Scott, T., Dodet, G., Suanez, S., Jackson, D., Floc'h, F., 2016a. Extreme wave activity during 2013/2014 winter and morphological impacts along the Atlantic coast of Europe. *Geophys. Res. Lett*., 43: 2135–2143, doi:10.1002/2015GL067492.

Masselink, G., Scott, T., Poate, T., Russell, P., Davidson, M., Conley, D., 2016b. The extreme 2013/2014 winter storms: Hydrodynamic forcing and coastal response along the southwest coast of England. *Earth Surf. Processes Landforms*, 41(3): 378–391, doi:10.1002/esp.3836.

Menendez, M., Mendez, F. J., Losada, I. J., Graham, N. E., 2008. Variability of extreme wave heights in the northeast Pacific Ocean based on buoy measurements. *Geophys. Res. Lett*., 35: L22607, doi:10.1029/2008GL035394.

Murray, R., Simmonds, I., 1991. A numerical scheme for tracking cyclone centres from digital data. Part I: Development and operation of the scheme. *Aust. Meteorol. Mag*., 39(3): 155–166.

Perez, J., Mendez, F. J., Menendez, M., Losada, I. J., 2014. ESTELA: A method for evaluating the source and travel time of the wave energy reaching a local area. *Ocean Dyn*., 64(8), 1181–1191, doi:10.1007/s10236-014-0740-7.

Pinto, J. G., Spangehl, T., Ulbrich, U., Speth, P., 2005. Sensitivities of a cyclone detection and tracking algorithm: Individual tracks and climatology. *Meteorol. Z*., 14(6), 823–838, doi:10.1127/0941-2948/2005/0068.

Robinet, A., Castelle, B., Idier, D., Le Cozannet, G., Déqué, M., Charles, E., 2016. Statistical modeling of interannual shoreline change driven by North Atlantic climate variability spanning 2000–2014 in the Bay of Biscay. *Geo-Mar. Lett.*, 36: 479–490, doi:10.1007/s00367-016-0460-8.

Rogers, J. C., 1981. Spatial variability of seasonal sea level pressure and 500 mb height anomalies. *Mon. Weather Rev.*, 109(10): 2093–2106.

Ruggiero, P., Komar, P. D., Allan, J. C., 2010. Increasing wave heights and extreme value projections: The wave climate of the US Pacific Northwest. *Coastal Eng.*, 57: 539–552.

Suanez, S., Cancouet, R., Floc'h, F., Blaise, E., Ardhuin, F., Filipot, J.-F., Cariolet, J.-M., Delacourt, C., 2015. Observations and predictions of wave runup, extreme water levels, and medium-term dune erosion during storm conditions. *J. Mar. Sci. Eng.*, 3(3): 674, doi:10.3390/jmse3030674.

Tolman, H. L., 2014. *User manual and system documentation of WAVEWATCH III version 4.18*, NOAA/NWS/NCEP/ MMAB Tech. Note 316, 194 pp., NOAA/NWS/NCEP/MMAB, College Park, Md.

Trenberth, K. E., Paolino, D. A., 1980. The Northern Hemisphere sea-level pressure data set: Trends, errors and discontinuities. *Mon. Weather Rev.*, 108(7): 855–872.